Available online at www.sciencedirect.com

ScienceDirect

Advances in Space Research 59 (2017) 1514–1525

ADVANCES IN SPACE RESEARCH (a COSPAR publication)

www.elsevier.com/locate/asr

Collision avoidance ZEM/ZEV optimal feedback guidance for powered descent phase of landing on Mars

Yao Zhang [a], Yanning Guo [a,*], Guangfu Ma [a], Tianyi Zeng [b]

[a] Department of Control Science and Engineering, Harbin Institute of Technology, Harbin 150001, China
[b] School of Automation, Beijing Institute of Technology, Beijing 100081, China

Received 8 June 2016; received in revised form 28 December 2016; accepted 30 December 2016
Available online 9 January 2017

Abstract

A novel zero-effort-miss (ZEM)/zero-effort-velocity (ZEV) optimal feedback guidance is proposed in order to rule out the possibility of Martian surface collision caused by the classical ZEM/ZEV optimal feedback guidance. The main approach is to add a collision avoidance term, which has self-adjustment capacity to ensure the near fuel optimality. Its main improvement is that it can not only successfully avoid collisions with the thruster constraint but also guarantee the near fuel optimality, and both of them are pivotal performances in Mars landing missions. Simulations are made to show the effectiveness of the proposed guidance and the parameters effects are simulated as well to analyze the properties of the proposed guidance.

Keywords: ZEM/ZEV method; Collision avoidance; Fuel-optimality; Powered descent phase; Mars landing

1. Introduction

Mars landing problems have been widely researched recently, and several engineering missions on Mars landing have been done (Braun and Manning, 2007), such as Viking, Spirit, Opportunity, and Phoenix missions. Mars landing process can be mainly decomposed into three phases, which are entry, descent and landing (EDL), respectively (Wells et al., 2006). Among them, the guidance for powered descent phase plays a vital role in precision landing missions as the final phase, which will determine the performance of the whole landing process.

The main problem in powered descent phase is to design a guidance which can ensure the precision landing and satisfy the fuel optimality. Researches on this problem mainly utilize the optimization methods to design the guidance and use the relevant software (GPOPS, TOMLAB, etc.) to obtain the optimal solutions. Among those optimization methods, convex optimization method has been used to design an optimal trajectory for Mars landing missions. Blackmore et al. (2010) proposed a Mars landing trajectory with minimum terminal errors using convex optimization method. Acikmese and Ploen (2007) designed a convex programming approach to give the numerical solution of fuel optimality. Rui et al. (2005) developed a multi-agent planning system, which can achieve onboard planning with minimum errors in deep space. Acikmese et al. (2008) advanced the fuel optimality guidance by taking certain constraints into account. Although convex optimization method has been proved effective in powered descent phase of Mars landing, it is an open loop guidance, whose performance will be reduced when disturbances exist, which means this method have no robustness. Therefore, to propose optimal feedback guidance is essential, which can

* Corresponding author at: Room 606, Main Building, Harbin Institute of Technology, No. 92 Xidazhi Street, Harbin, China.
E-mail addresses: yaozhanghit@outlook.com (Y. Zhang), guoyn@hit.edu.cn (Y. Guo), magf@hit.edu.cn (G. Ma), tyzeng0525@outlook.com (T. Zeng).

http://dx.doi.org/10.1016/j.asr.2016.12.040
0273-1177/

guarantee the fuel optimality and satisfy the needs of precision landing with certain constraints.

The classical ZEM ZEV optimal feedback guidance has been widely used in missile interception, space rendezvous and docking and planetary landing problems due to its unique advantages of high accuracy, easy to design and clear physical meaning (Ebrahimi et al., 2008). The concepts of ZEM and ZEV were proposed firstly by Ebrahimi et al., who used this method to design optimal sliding mode guidance with terminal velocity constraints. Furfaro et al. (2011) advanced ZEM/ZEV method and applied it to precision lunar landing problems, which can ensure the pinpoint landing with thrusters limits. Wibben and Furfaro (2015) proposed a ZEM/ZEV optimal sliding guidance algorithm for Mars powered descent phase, which exhibited a higher degree of robustness and flexibility. Guo et al. (2013a,b) generated an improved ZEM/ZEV feedback guidance algorithm, which simplified the guidance expression. Guo et al. (2013a,b) designed ZEM/ZEV feedback guidance for Mars landing based on waypoint optimization to reduce the online calculation amount. Although the effectiveness of the classical ZEM/ZEV method has been proven in Mars landing missions, the altitude constraint is not taken into consideration, which in some cases will make the lander crash on the Martian surface.

In order to address collision problems, Neveu et al. (2005) developed a hazard-avoidance method using closed-loop software simulator tools, which had good performance to avoid collisions, while it cannot be applied to many scenarios due to the calculation amount limitation. Johnson et al. (2002) designed a method to avoid hazards by processing scanning lidar data to find safe landing sites, while the fuel optimality cannot be satisfied. Wong et al. (2002) proposed automated hazard avoidance guidance by solving a two-point boundary-value problem, whereas the fuel consumption was not discussed. Zhou and Xia (2014) proposed an improved ZEM/ZEV feedback guidance for Mars powered descent phase by adding a switching-form term which was relevant to the lander's position, and it was proved effective with good performance in avoiding collisions, while the added term mainly relies on the expert experience, which may reduce the reliability to some extent and cannot ensure the near fuel optimality. Therefore, it is necessary to design a feedback guidance which does not depend on the expert experience and has the self-adjustment ability to ensure near fuel optimality.

Collision avoidance ZEM/ZEV optimal feedback guidance is proposed in this paper, which takes the altitude constraint into account and design a collision avoidance term to ensure there is no Martian surface crash, more importantly, the collision avoidance term has self-adjustment ability to guarantee the fuel optimality. Furthermore, the precision landing is ensured under the proposed algorithm with thrust constraints and certain disturbances.

The rest of this paper is organized as follows. Preliminary knowledge is introduced in Section 2. Detailed information of the proposed algorithm is given in Section 3 including the derivational process and analysis. Section 4 is the simulation part, which is decomposed into three sub-sections to show the effectiveness and the parameters effect. We conclude this paper in Section 5.

2. Problem formulation

2.1. Mathematical model

At the first entry in powered descent phase, the relative distance between the lander and the Martian surface is within five kilometers, and the relative velocity is within several hundred meters per second, so that the atmosphere drag can be ignored.

The coordinate frame to describe dynamics and kinematics is a nonrotating inertial coordinate frame fixed on the Martian surface with its origin at the target landing site, which is shown in Fig. 1.

The mathematical model of the lander during this phase can be expressed in the surface fixed coordinate frame as

$$\begin{cases} \dot{\boldsymbol{r}} = \boldsymbol{v} \\ \dot{\boldsymbol{v}} = \boldsymbol{a} + \boldsymbol{g} \\ \boldsymbol{a} = \boldsymbol{F}/m \\ \dot{m} = -|\boldsymbol{F}|/c_p \end{cases} \tag{1}$$

where $\boldsymbol{r} = [r_x, r_y, r_z]^T$, $\boldsymbol{v} = [v_x, v_y, v_z]^T$ and $\boldsymbol{a} = [a_x, a_y, a_z]^T$ denote the position vector, velocity vector and control acceleration vector (supplied by thrusters) of the lander, respectively, and $\boldsymbol{g} = [0, 0, g]^T$ is the gravitational acceleration vector, which is considered as a constant since the altitude's variation is small enough to be ignored during

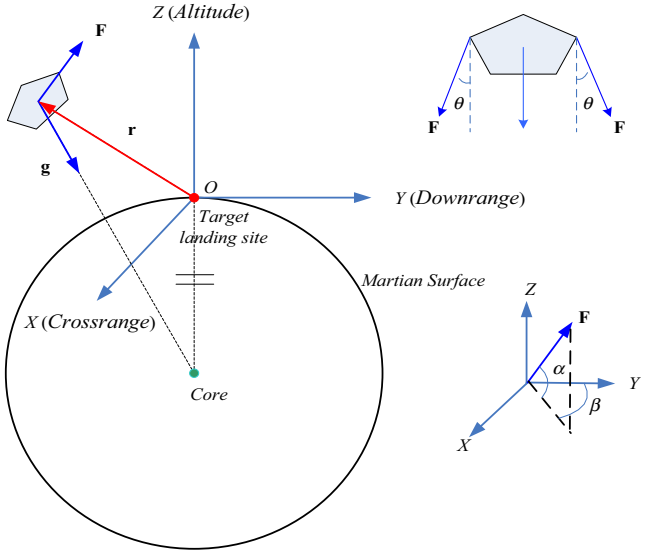

Fig. 1. Surface fixed coordinate frame.

powered descent phase, m is the lander's mass, and c_p is the engine exhaust velocity represented by $c_p = I_{sp}g_e$, where I_{sp} is the thrusters' impulse and g_e is earth's gravitational acceleration, $\boldsymbol{F} = [F_x, F_y, F_z]^T$ denotes the thrusting force acting on the lander with following expression:

$$\boldsymbol{F} = \begin{bmatrix} F_x \\ F_y \\ F_z \end{bmatrix} = \begin{bmatrix} |\boldsymbol{F}| \cos\alpha \sin\beta \\ |\boldsymbol{F}| \cos\alpha \cos\beta \\ |\boldsymbol{F}| \sin\alpha \end{bmatrix} \tag{2}$$

where $|\boldsymbol{F}| = nkF_m \cos\theta$ denotes the two-norm of $\boldsymbol{F}$, n represents the thruster number, k is the throttle level of each thruster, F_m is the maximum force, which can be provided by one thruster, and θ denotes the angle between actual thrust and net thrust as shown in Fig. 1. The thruster constraint is considered according to (Acikmese and Ploen, 2007), which is

$$0.3F_m \leqslant |\boldsymbol{F}| \leqslant 0.8F_m \tag{3}$$

During the powered descent phase, in order to avoid collision completely, we set an index δ, which denotes the minimum safety distance between the lander and the Martian surface along the altitude axis, and its value should be set as a positive constant.

2.2. ZEM and ZEV description

Zero effort miss (ZEM) is defined as Eq. (4), whose physical significance is the errors between the target position $\boldsymbol{r}_f$ and the final position $\boldsymbol{r}(t_f)$ with no command input after the current time till $t = t_f$.

$$\boldsymbol{ZEM}(t) = \boldsymbol{r}_f - \boldsymbol{r}(t_f) \tag{4}$$

Zero effort velocity (ZEV) is defined as (5), whose physical significance is the errors between target velocity $\boldsymbol{v}_f$ and the final velocity $\boldsymbol{v}(t_f)$ with no command input after the current time until $t = t_f$.

$$\boldsymbol{ZEV}(t) = \boldsymbol{v}_f - \boldsymbol{v}(t_f) \tag{5}$$

In this problem, $\boldsymbol{r}(t_f)$ and $\boldsymbol{v}(t_f)$ can be expressed as

$$\boldsymbol{r}(t_f) = \boldsymbol{r} + t_{go}\boldsymbol{v} + \int_t^{t_f} (t_f - \tau)\boldsymbol{g}(\tau)d\tau \tag{6}$$

$$\boldsymbol{v}(t_f) = \boldsymbol{v} + \int_t^{t_f} \boldsymbol{g}(\tau)d\tau \tag{7}$$

where t_{go} is time-to-go with definition of $t_{go} = t_f - t$.

Under the assumption that gravitational acceleration $\boldsymbol{g} = [0, 0, g]^T$ can be treated as a constant vector, the ZEM/ZEV descriptions are shown in Eqs. (8) and (9).

$$\boldsymbol{ZEM}(t) = \boldsymbol{r}_f - \boldsymbol{r}(t_f) = \boldsymbol{r}_f - \left[\boldsymbol{r} + t_{go}\boldsymbol{v} + \frac{1}{2}t_{go}^2\boldsymbol{g}\right] \tag{8}$$

$$\boldsymbol{ZEV}(t) = \boldsymbol{v}_f - [\boldsymbol{v} + t_{go}\boldsymbol{g}] \tag{9}$$

3. Collision avoidance ZEM/ZEV optimal feedback guidance

In this section, collision avoidance ZEM/ZEV optimal feedback guidance is proposed by advance the classical ZEM/ZEV algorithm, in which the performance index is designed as

$$J = \frac{1}{2}\int_{t_0}^{t_f} \boldsymbol{a}^T\boldsymbol{a}dt \tag{10}$$

subjected to Eq. (1) and with the boundary conditions of initial state and terminal state, the Hamiltonian function is defined as

$$H = \frac{1}{2}\boldsymbol{a}^T\boldsymbol{a} + \boldsymbol{p}_r^T\boldsymbol{v} + \boldsymbol{p}_v^T(\boldsymbol{a} + \boldsymbol{g}) \tag{11}$$

where $\boldsymbol{p}_r$ and $\boldsymbol{p}_v$ are the costate vectors associated with the position and velocity vectors, respectively. The command acceleration is expressed as

$$\boldsymbol{a} = \frac{6}{t_{go}^2}\boldsymbol{ZEM} - \frac{2}{t_{go}}\boldsymbol{ZEV} \tag{12}$$

It can be seen that for the ZEM/ZEV optimal feedback guidance, the value of t_f plays an important role. Current researches investigate the relationship between t_f and fuel consumption or the control effort, and determine the value of t_f by minimizing the fuel usage (Zhou and Xia, 2014) or the control effort (Guo et al., 2011). However, these t_f determination methods will cause collisions in some cases (shown in Fig. 2), which will lead to the whole mission failure. If t_f is chosen as a small value, the lander will not arrive at the target landing site, because even if the maximum thrust is added, the lander cannot reach the target landing site due to the short time. If t_f is chosen as a big value, the trajectory of the lander will have underground part. An example to show the effect of t_f is shown in Fig. 2, and the initial position is $\boldsymbol{r}_0 = [-2000; 0; 1500]$ m and t_f is set as a range of value: $t_f = 30{:}5{:}100$ s.

It can be seen that under different values of the initial velocity, some values of t_f make the trajectories have underground part and some cannot make the lander complete the landing missions. Therefore, it is necessary to propose an optimal feedback guidance, which can ensure no collisions under a range of t_f values.

In classical ZEM/ZEV optimal feedback guidance, the collision phenomenon will exist since the altitude constraint is not considered. In order to rule out all of the possibilities of collisions and guarantee the fuel-optimality, a novel performance index is designed in this section, which employs the lander's states to adjust the additional term.

The novel performance index is

$$J = \frac{1}{2}\int_{t_0}^{t_f} \left(\boldsymbol{a}^T\boldsymbol{a} - \frac{c}{r_z^2 + \varphi}\boldsymbol{Ar}\right)dt \tag{13}$$

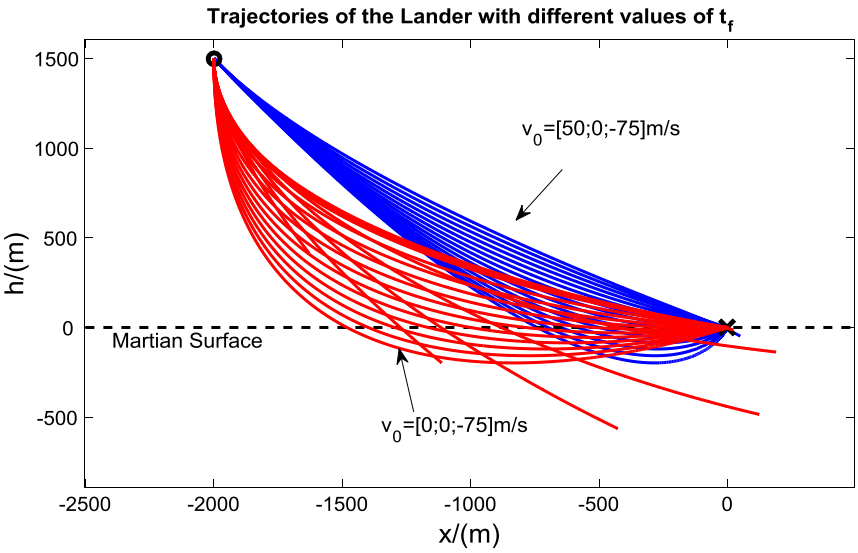

Fig. 2. Trajectories under different initial velocities and values of t_f.

where $c > 0$ is a constant parameter, $\boldsymbol{A} = [0, 0, 1]$, r_z is the component of the position vector in altitude direction, $\varphi = \frac{\delta^2}{3}$, and δ denotes the minimum safety distance.

Remark 1. The term of $-\frac{c}{r_z^2+\varphi}\boldsymbol{Ar}$ is added to the performance index Eq. (13), which is desired to be minimized in optimization problem and the solutions can be obtained by utilizing Hamiltonian function. Since the purpose of this algorithm is to minimize the performance index's value, when the term of $-\frac{c}{r_z^2+\varphi}\boldsymbol{Ar}$ — a negative value is added into Eq. (13), there will be an extra force with upwards direction automatically, consequently, it can avoid the lander crashing on the Martian surface. Furthermore, because the avoid-collisions-term is only added in the altitude direction, so the classical ZEM/ZEV optimal feedback guidance is used in other two directions.

Remark 2. Note that the value of $\frac{c}{r_z^2+\varphi}\boldsymbol{Ar}$ is relatively small at the beginning of the powered descent phase since the value of r_z^2 is relatively big, which means that the term of $-\frac{c}{r_z^2+\varphi}\boldsymbol{Ar}$ affects little to ensure the fuel-optimality. Then as the altitude-direction distance between the lander and Martian surface gets smaller, the value of $\frac{c}{r_z^2+\varphi}\boldsymbol{Ar}$ becomes bigger, which makes the term of $-\frac{c}{r_z^2+\varphi}\boldsymbol{Ar}$ play an increasing role to avoid collisions. If the minimum safety distance arrives, the term of $-\frac{c}{r_z^2+\varphi}\boldsymbol{Ar}$ will makes the thrusters provide the maximum force. Afterwards, the term of $-\frac{c}{r_z^2+\varphi}\boldsymbol{Ar}$ will affects less as the lander goes upwards to guarantee the fuel-optimality.

The Hamiltonian function is defined in the following form,

$$H = \frac{1}{2}\boldsymbol{a}^T\boldsymbol{a} - \frac{1}{2}\frac{c}{r_z^2+\varphi}\boldsymbol{Ar} + \boldsymbol{p}_r^T\boldsymbol{v} + \boldsymbol{p}_v^T(\boldsymbol{a}+\boldsymbol{g}) \tag{14}$$

The optimal control equation is

$$\frac{\partial H}{\partial \boldsymbol{a}} = 0 \tag{15}$$

and its solution is

$$\boldsymbol{a} = -\boldsymbol{p}_v \tag{16}$$

The costate equations are as follows

$$\dot{\boldsymbol{p}}_r = -\frac{\partial H}{\partial \boldsymbol{r}} = \frac{A^T c}{2}\cdot\frac{r_z^2-\varphi}{\left[r_z^2+\varphi\right]^2} \tag{17}$$

$$\dot{\boldsymbol{p}}_v = -\frac{\partial H}{\partial \boldsymbol{v}} = -\boldsymbol{p}_r \tag{18}$$

Note that before the lander reaches the lowest point in the altitude direction, its altitude is keeping declining, i.e. $\dot{r}_z \leqslant 0$ and $\ddot{\boldsymbol{p}}_r \geqslant 0$ if $r_z \geqslant \delta$. So we can get that

$$\boldsymbol{p}_r \leqslant \boldsymbol{p}_r(t_f) - t_{go}\cdot\dot{\boldsymbol{p}}_r \tag{19}$$

In order to get guidance in simple form, we can treat $\boldsymbol{p}_r$ as $\boldsymbol{p}_r = \boldsymbol{p}_r(t_f) - t_{go}\cdot\dot{\boldsymbol{p}}_r$, because if we select the command acceleration as its maximum value, it will achieve the best performance of avoiding collisions.

Then we solve $\boldsymbol{p}_r$ and $\boldsymbol{p}_v$ by utilizing their derivatives Eqs. (17) and (18) respectively, and the results are as follows:

$$\boldsymbol{p}_r = \boldsymbol{p}_r(t_f) - t_{go}\cdot\boldsymbol{A}^T\cdot\frac{c}{2}\cdot\frac{r_z^2-\varphi}{\left[r_z^2+\varphi\right]^2} \tag{20}$$

$$\boldsymbol{p}_v = \boldsymbol{p}_v(t_f) + t_{go}\boldsymbol{p}_r(t_f) - t_{go}^2\cdot\frac{\boldsymbol{A}^T c}{4}\cdot\frac{r_z^2-\varphi}{\left[r_z^2+\varphi\right]^2} \tag{21}$$

According to Eq. (16), the command acceleration can be written as

$$\boldsymbol{a} = -\boldsymbol{p}_v(t_f) - t_{go}\boldsymbol{p}_r(t_f) + t_{go}^2\cdot\frac{\boldsymbol{A}^T c}{4}\cdot\frac{r_z^2-\varphi}{\left[r_z^2+\varphi\right]^2} \tag{22}$$

By integrating the whole acceleration, which is expressed as $(\boldsymbol{a}+\boldsymbol{g})$, we can obtain the velocity vector and position vector in the following form:

$$\boldsymbol{v}=\boldsymbol{v}_f-t_{go}^3\cdot\frac{\boldsymbol{A}^T c}{12}\cdot\frac{r_z^2-\varphi}{\left[r_z^2+\varphi\right]^2}+\frac{1}{2}t_{go}^2\boldsymbol{p}_r(t_f)+t_{go}\boldsymbol{p}_v(t_f)-t_{go}\boldsymbol{g} \tag{23}$$

$$\boldsymbol{r}=\boldsymbol{r}_f+t_{go}^4\cdot\frac{\boldsymbol{A}^T c}{48}\cdot\frac{r_z^2-\varphi}{\left[r_z^2+\varphi\right]^2}-\frac{1}{6}t_{go}^3\boldsymbol{p}_r(t_f)-\frac{1}{2}t_{go}^2\boldsymbol{p}_v(t_f)+\frac{1}{2}t_{go}^2\boldsymbol{g}-t_{go}\boldsymbol{v}_f \tag{24}$$

Combining Eqs. (23) and (24) leads to

$$\boldsymbol{p}_r(t_f)=\frac{6(\boldsymbol{v}_f+\boldsymbol{v})}{t_{go}^2}+\frac{12(\boldsymbol{r}-\boldsymbol{r}_f)}{t_{go}^3}+t_{go}\cdot\frac{\boldsymbol{A}^T c}{4}\cdot\frac{r_z^2-\varphi}{\left[r_z^2+\varphi\right]^2} \tag{25}$$

$$\boldsymbol{p}_v(t_f)=-\frac{4\boldsymbol{v}_f+2\boldsymbol{v}}{t_{go}}-\frac{6(\boldsymbol{r}-\boldsymbol{r}_f)}{t_{go}^2}+\boldsymbol{g}-t_{go}^2\cdot\frac{\boldsymbol{A}^T c}{24}\cdot\frac{r_z^2-\varphi}{\left[r_z^2+\varphi\right]^2} \tag{26}$$

Substitute Eqs. (25) and (26) into Eq. (22), the collision avoidance guidance is calculated as

$$\boldsymbol{a}=\frac{6[\boldsymbol{r}_f-(\boldsymbol{r}+t_{go}\boldsymbol{v})]}{t_{go}^2}-\frac{2(\boldsymbol{v}_f-\boldsymbol{v})}{t_{go}}-\boldsymbol{g}+t_{go}^2\cdot\frac{\boldsymbol{A}^T c}{24}\cdot\frac{r_z^2-\varphi}{\left[r_z^2+\varphi\right]^2} \tag{27}$$

To obtain the collision avoidance guidance in the form of ZEM/ZEV, Eqs. (8) and (9) are utilized, and the collision avoidance ZEM/ZEV optimal feedback guidance for powered descent phase of landing on Mars is as follows

$$\boldsymbol{a}=\frac{6}{t_{go}^2}\boldsymbol{ZEM}-\frac{2}{t_{go}}\boldsymbol{ZEV}+t_{go}^2\cdot\frac{\boldsymbol{A}^T c}{24}\cdot\frac{r_z^2-\varphi}{\left[r_z^2+\varphi\right]^2} \tag{28}$$

Remark 3. Compared with the classical ZEM/ZEV optimal feedback guidance Eq. (12), the proposed guidance Eq. (28) adds a term of $t_{go}^2\cdot\frac{\boldsymbol{A}^T c}{24}\cdot\frac{r_z^2-\varphi}{\left[r_z^2+\varphi\right]^2}$, which can be treated as a collision avoidance term and is in accordance with the performance index design objective.

3.1. Analysis

Defining a new vector $\boldsymbol{\psi}_{ca}=t_{go}^2\cdot\frac{\boldsymbol{A}^T c}{24}\cdot\frac{r_z^2-\varphi}{\left[r_z^2+\varphi\right]^2}$, and $\boldsymbol{\psi}_{ca}$ denotes the collision avoidance term. The projections of $\boldsymbol{\psi}_{ca}$ and $\boldsymbol{r}$ along the z-axis (altitude direction) are defined as ψ_{caz} and r_z respectively.

The partial derivative of ψ_{caz} to r_z can be expressed as

$$\frac{\partial\psi_{caz}}{\partial r_z}=\frac{\partial}{\partial r_z}\left[\frac{t_{go}^2\cdot c}{24}\cdot\frac{r_z^2-\varphi}{(r_z^2+\varphi)^2}\right]=\frac{t_{go}^2\cdot c}{12}\cdot\frac{-2r_z^3+6r_z\varphi}{(r_z^2+\varphi)^3} \tag{29}$$

Substitute $\varphi=\frac{\delta^2}{3}$ into Eq. (29), we can obtain

$$\frac{\partial\psi_{caz}}{\partial r_z}=\frac{t_{go}^2\cdot c}{6}\cdot\frac{-r_z^3+r_z\delta^2}{(r_z^2+\varphi)^3} \tag{30}$$

From (30), the extreme points can be calculated, which are $r_z=\delta$ and $r_z=0$, and we analyze the proposed collision avoidance guidance as follows:

(1) From the initial position to the minimum safety distance point, which is $r_z: r_z(0)\to\delta$.

In this phase, the collision avoidance term ψ_{caz} is a reduction function of the variable r_z, which means the collision avoidance term will provide a bigger command acceleration when the distance between lander and Martian surface becomes smaller, on the other hand, if the lander is far away from the Martian surface, the collision avoidance term is small enough to guarantee the optimality of fuel usage.

(2) At the minimum safety distance point, which is $r_z=\delta$.

At this point, the collision avoidance term arrives at the maximum value, which means that the thrusters will provide a maximum force to make the lander be away from the Martian surface when the lander arrives at the minimum safety distance point.

4. Simulation results

In this section, we will test the properties of the proposed guidance by three steps.

Firstly, the collision avoidance ability will be verified by comparing with the classical ZEM/ZEV optimal feedback guidance (Acikmese and Ploen, 2007).

Secondly, owing to the self-adjustment ability, the proposed guidance has the near fuel optimality property, which will be tested by comparing with another collision avoidance method (Zhou and Xia, 2014).

Thirdly, in order to investigate how the parameters influence the performance of the proposed guidance, some simulations and analysis will be made.

Parameters about the lander are designed as the simulation conditions introduced in Acikmese and Ploen (2007) and Zhou and Xia (2014) which are as follows,

Initial mass: $m_0=1905$ kg;
Number of thrusters: $n=6$;
Included angle: $\theta=27^\circ$;
Thrusters' impulsive: $I_{sp}=225$ s;
Maximum force (one thruster): $F_m=3.1$ kN.

And the parameters of gravitational accelerations on Mars and earth are:
Mars: $g=[0\quad 0\quad -3.7114]^T$ m/s^2;
Earth: $g_e=9.807$.

Due to the soft landing demands, the following terminal states should be satisfied:

$$\boldsymbol{r}(t_f) = [0 \quad 0 \quad 0]^T \text{ m};$$

$$\boldsymbol{v}(t_0) = [0 \quad 0 \quad 0]^T \text{ m/s}.$$

The flight time is set as $t_f = 100$ s. The minimum value of t_f, which permits a soft landing for a lander equipped with thrust-limited engines, can be obtained by Eq. (31).

$$t_{f\min} = \max\left\{\frac{-v_z(0)}{a_{\max} - g}, \frac{-v_z(0) + \sqrt{v_z^2(0) - 2a_{\max}r_z(0)}}{a_{\max}}\right\} \tag{31}$$

4.1. Simulations on effectiveness of avoiding collision

In this part, in order to show the robustness and reliability of the proposed guidance, the trajectories of the classical and the proposed ZEM/ZEV algorithms are simulated by Monte Carlo Method.

Monte Carlos with 300 cases and varying initial states are run using Matlab simulation. The initial dispersions are listed in Table 1, which is consistent with the Table 1 in Zhou and Xia (2014). Furthermore, the total perturbation constituted by the model uncertainty, the atmosphere disturbance, etc. is equivalent to a perturbation acceleration $\boldsymbol{a_p}$, where $\boldsymbol{a_p} = 0.2\boldsymbol{a}\sin\left(\frac{\pi}{3}t\right)$, and this assumption is same with Zhou and Xia (2014) as well.

The parameters in the proposed algorithm are $\delta = 1$ m and $c = 30$. Note that the minimum safe distance δ is set as a small value in order to test the effectiveness of the proposed guidance, and a larger value will be more practical to avoid the lander being much too close to the surface.

The trajectories (xoy plane projection) under the classical and the proposed ZEM/ZEV optimal feedback guidance are shown in Figs. 3 and 4, respectively. The final landing sites (xoy plane projection) under these two guidance are displayed in Figs. 5 and 6, respectively. It can be seen from Figs. 3–6 that there is no significant difference between these two guidance in the directions of crossrange and downrange, because in these two directions, no additional terms are added, and the little differences are caused by the disturbance.

The main improvement should be displayed in the altitude direction, especially the collision avoidance ability.

Table 1
Initial perturbations.

Initial perturbations	Mean value	Standard dev.
Altitude position	1500 m	100 m
Crossrange position	0 m	50 m
Downrange position	−2000 m	150 m
Altitude velocity	−75 m/s	5 m/s
Crossrange velocity	0 m/s	10 m/s
Downrange velocity	100 m/s	10 m/s
Mass	1905 kg	30 kg

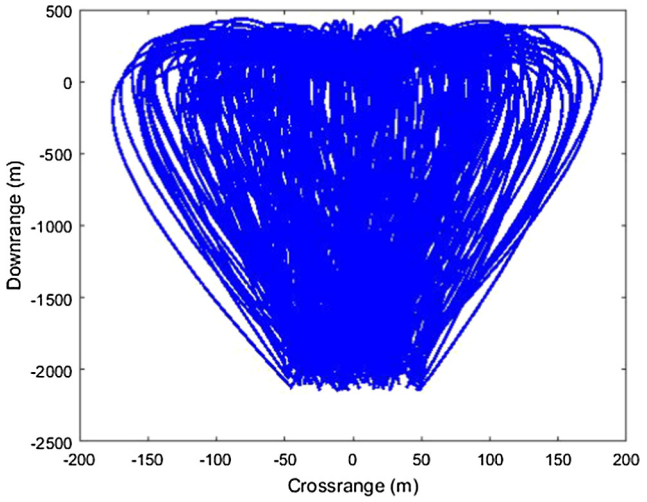

Fig. 3. Trajectories of the classical ZEM/ZEV Optimal Feedback Guidance.

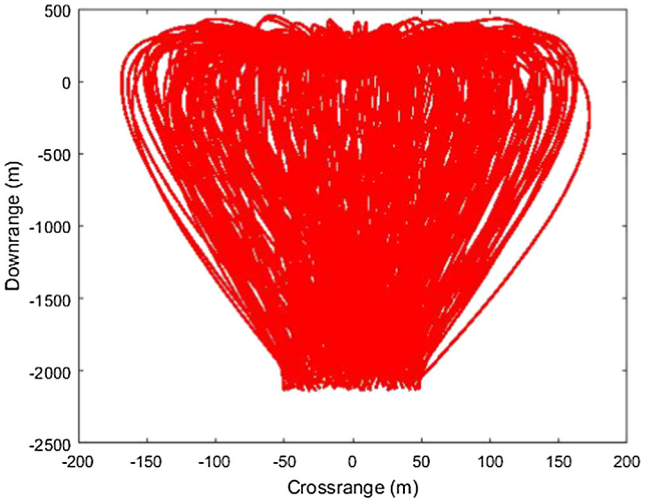

Fig. 4. Trajectories of the proposed ZEM/ZEV Optimal Feedback Guidance.

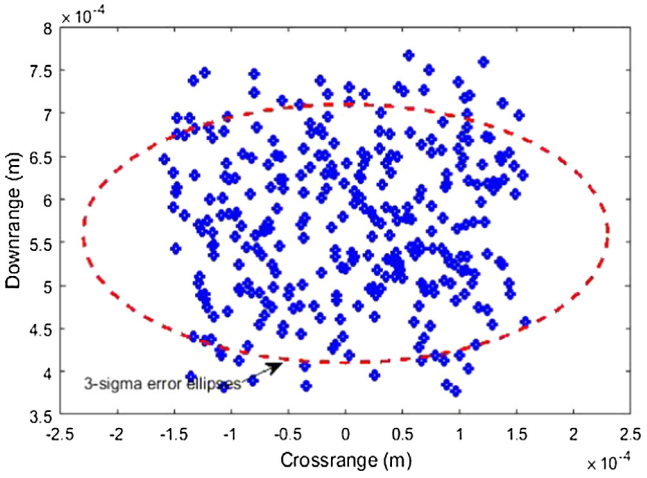

Fig. 5. Final landing sites of the classical ZEM/ZEV Optimal Feedback Guidance.

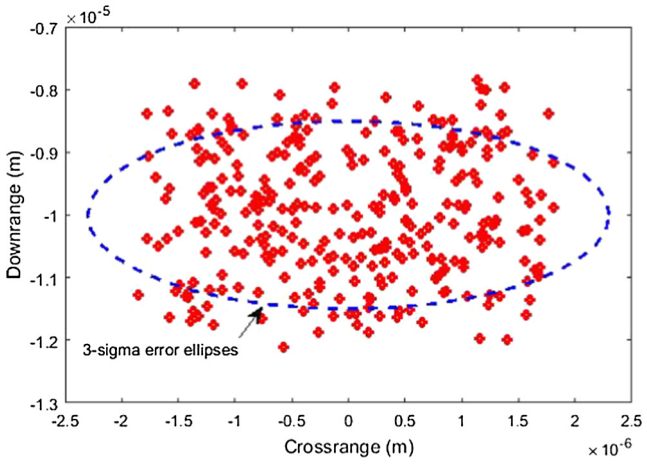

Fig. 6. Final landing sites of the proposed ZEM/ZEV Optimal Feedback Guidance.

The trajectories and velocities in altitude direction under the classical and proposed ZEM/ZEV optimal feedback guidance are indicated in Figs. 7–12, respectively. From Fig. 7, we can find that although the classical guidance can lead the lander to the target landing site, there are collisions in most cases. From Fig. 8, it can be found that the proposed guidance can effectively avoid the lander crash on the Martian surface, and the precision landing destination can be achieved. Figs. 11 and 12 show the velocities in downrange and crossrange directions under two guidance.

Therefore, the collision avoidance ability of the proposed guidance is verified by Monte Carlos simulations.

The landing statistics of this Monte Carlos simulation of two guidance are summed in Tables 2 and 3. It can be seen that the final landing sites of the proposed guidance are closer than the ones of the classical guidance, which verifies the effectiveness and superiority of the proposed guidance.

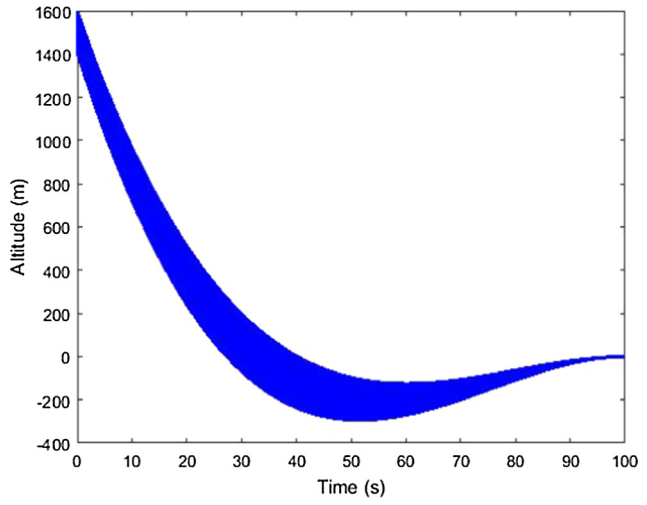

Fig. 7. Altitudes under the classical ZEM/ZEV Optimal Feedback Guidance.

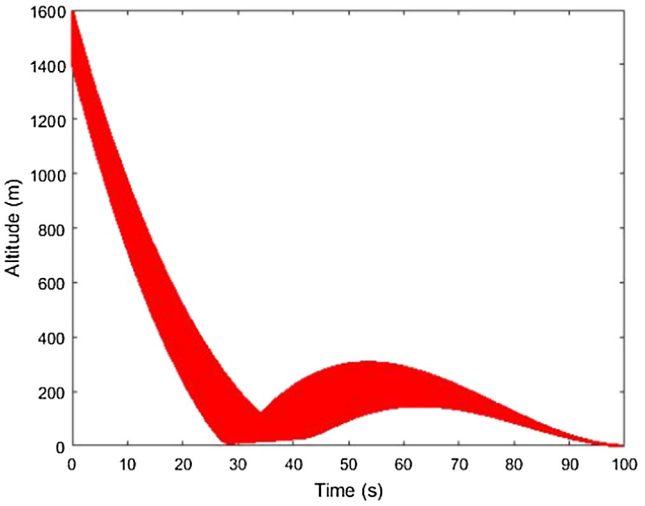

Fig. 8. Altitudes under the proposed ZEM/ZEV Optimal Feedback Guidance.

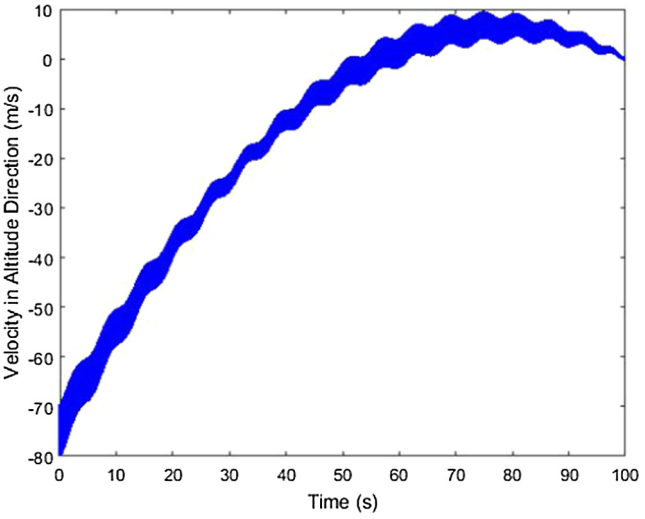

Fig. 9. Velocity in altitude direction under the Classical Guidance.

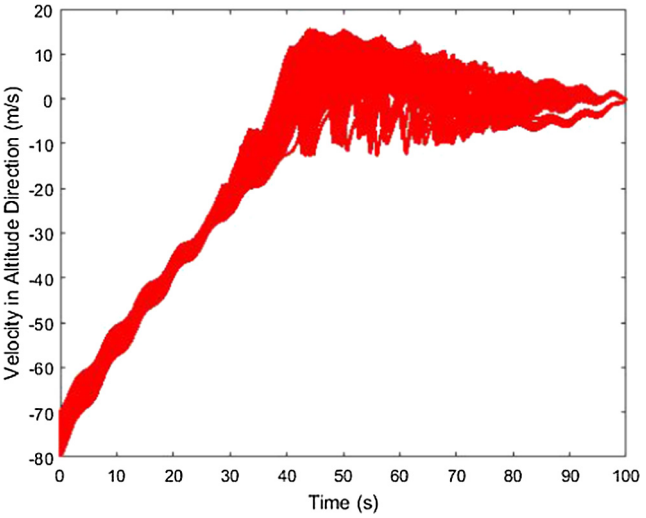

Fig. 10. Velocity in altitude direction under the Proposed Guidance.

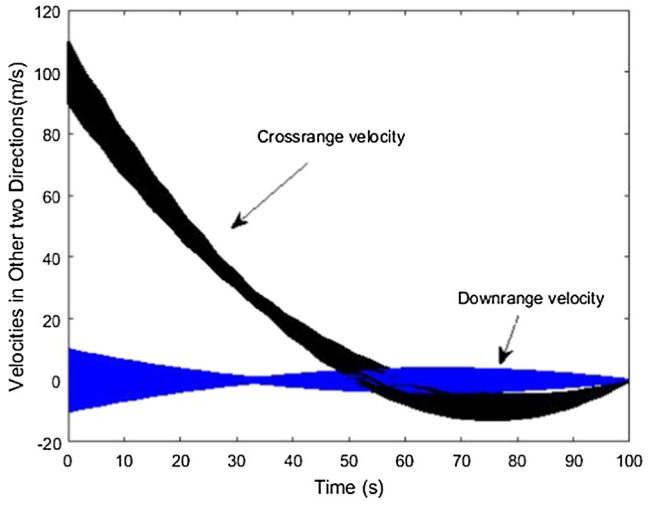

Fig. 11. Velocity in other two directions under classical ZEM/ZEV Optimal Feedback Guidance.

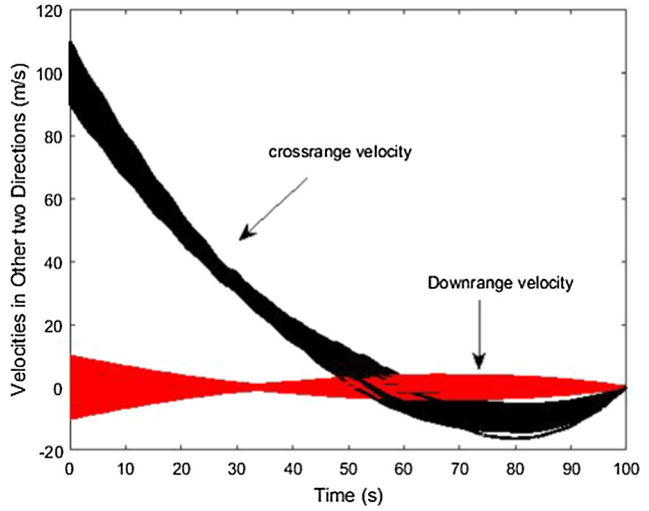

Fig. 12. Velocity in other two directions under proposed ZEM/ZEV Optimal Feedback Guidance.

Table 2
Landing statistics with the classical guidance.

Landing statistics	Mean value	Standard dev.
Altitude position	3.1746×10^{-5} m	1.7509×10^{-4} m
Crossrange position	2.7019×10^{-5} m	1.6431×10^{-4} m
Downrange position	5.7782×10^{-4} m	2.8042×10^{-4} m
Altitude velocity	-1.6×10^{-3} m/s	5.3×10^{-3} m/s
Crossrange velocity	2.3×10^{-3} m/s	6.6×10^{-3} m/s
Downrange velocity	-1.2×10^{-3} m/s	1.2×10^{-2} m/s

4.2. Simulations on near fuel optimality

In this part, the proposed guidance will be compared with the collision avoidance guidance introduced in Zhou and Xia (2014) in order to illustrate that although the guidance in Zhou and Xia (2014) can achieve collision avoidance, it cannot ensure the near fuel optimality.

Table 3
Landing statistics with the proposed guidance.

Landing statistics	Mean value	Standard dev.
Altitude position	9.7876×10^{-6} m	8.7439×10^{-5} m
Crossrange position	1.8342×10^{-7} m	9.6241×10^{-6} m
Downrange position	5.6383×10^{-6} m	4.8742×10^{-5} m
Altitude velocity	-1.1×10^{-3} m/s	3.5×10^{-3} m/s
Crossrange velocity	1.7×10^{-3} m/s	2.9×10^{-3} m/s
Downrange velocity	-4.5×10^{-3} m/s	2.3×10^{-2} m/s

The fuel usages under the classical guidance, the guidance in Zhou and Xia (2014) and the proposed guidance are shown in Fig. 13. It can be seen from Fig. 13 that the proposed guidance has near fuel optimality property, and the guidance in Zhou and Xia (2014) consumes the most usage, and this simulation result verifies the self-adjustment ability of the proposed guidance. Note that the t_f is selected by minimize another performance index in Zhou and Xia (2014) to guarantee the fuel optimality, which is more complex, because in this paper, the near fuel optimality can be ensured for any other proper values of t_f.

4.3. Simulations on parameters effect

In this part, control variable method is used to illustrate how each parameter affects the proposed algorithm performance. The classical ZEM/ZEV algorithm and the proposed one are compared under a specific initial state, which is selected as those introduced in Acikmese and Ploen (2007) as follows:

$$\boldsymbol{r}(t_0) = [0 \quad 2000 \quad 1500]^T \text{ m};$$

$$\boldsymbol{v}(t_0) = [0 \quad 100 \quad -75]^T \text{ m/s}.$$

(1) Parameter c

The parameter of proposed algorithm is $\delta = 1$ m, and we set c as a range of values: $c = 0, 30, 50, 100, 500$.

The simulation results are as follows.

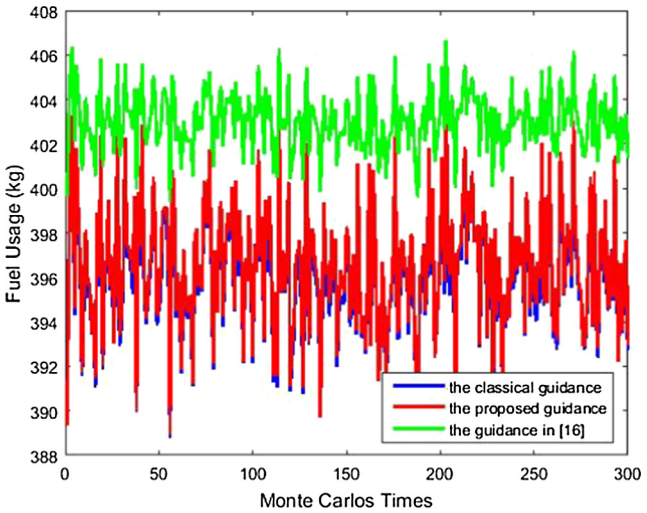

Fig. 13. Fuel usages under three guidance.

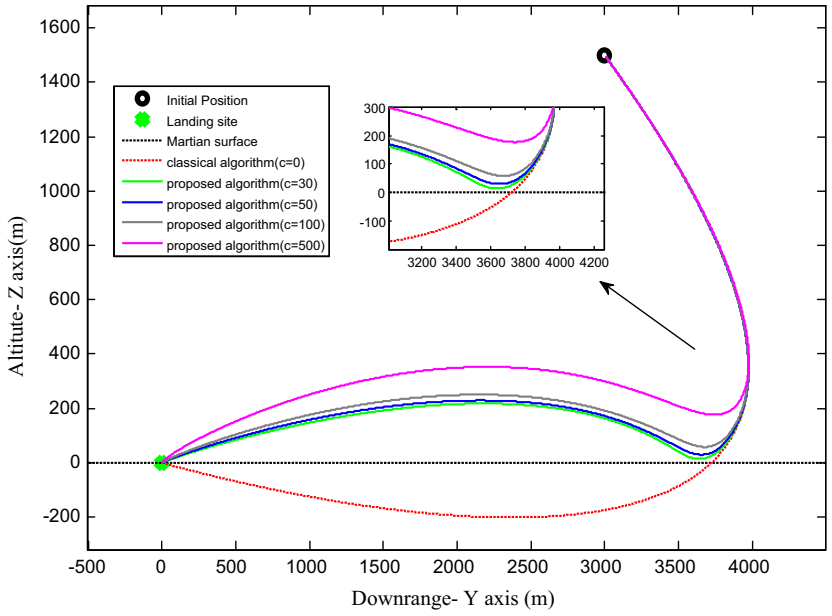

Fig. 14. Trajectories of classical algorithm and the proposed algorithm (under different c).

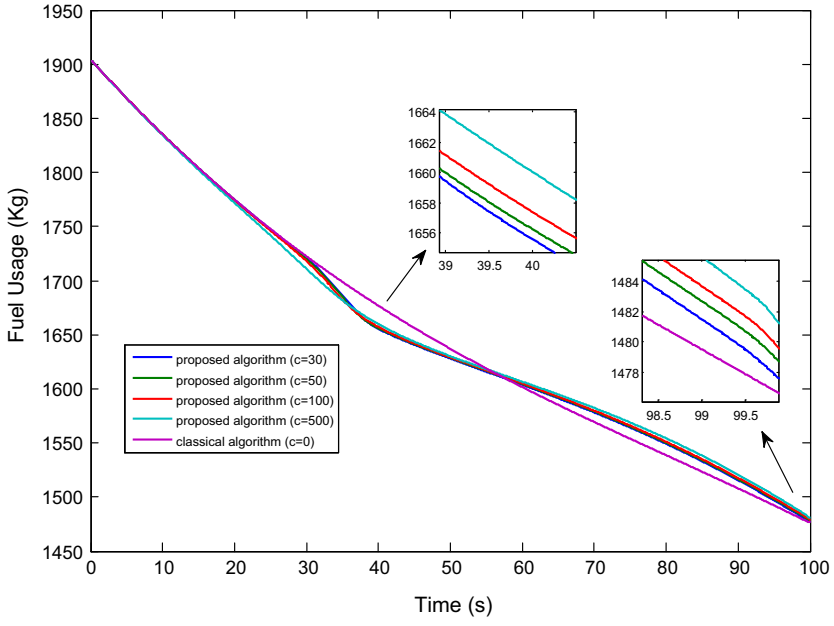

Fig. 15. Fuel usage under classical and proposed algorithms.

From Fig. 14 above, the effectiveness of the proposed algorithm is confirmed. The minimum distance between the lander and the Martian surface becomes larger when the value of c is bigger, for the reason that ψ_{caz} affects the trajectory more under this situation. From Fig. 15, we can see that the proposed algorithm consumes more fuel than the classical algorithm in the middle of the whole landing process, whereas the consumption of the proposed algorithm becomes less than the classical algorithm afterwards. The reason is that when the lander motions in the opposite direction of the Martian gravitational direction, the thrusters must provide thrust for resistance, during which process the fuel is used. Note that there are so small differences between two algorithms that no more than 5 kg is found.

(2) Parameter δ

The parameter of proposed algorithm is $c = 30$, and we set the minimum safety distance as a range of values: $\delta = 1, 5, 10, 15$ m.

The simulation results are as follows.

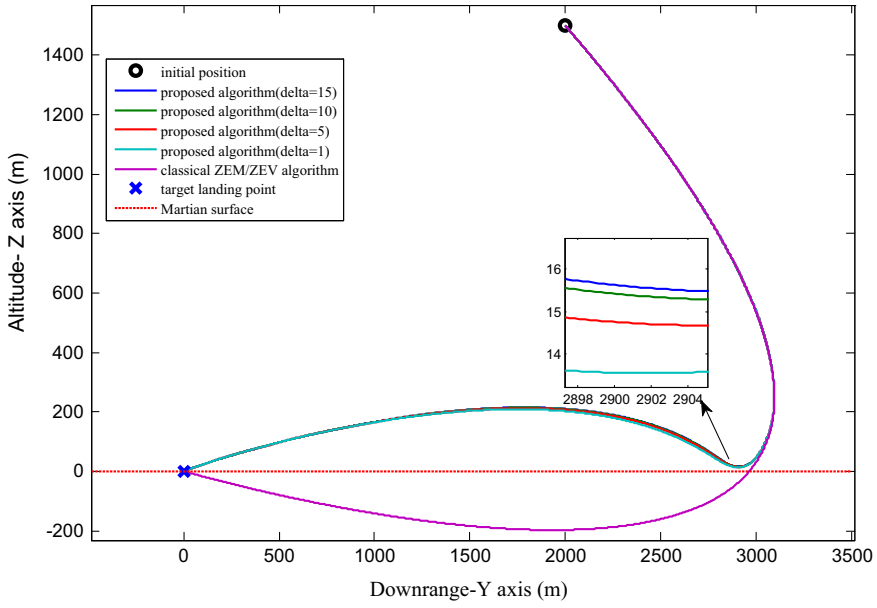

Fig. 16. Trajectories of classical algorithm and the proposed algorithm (under different δ).

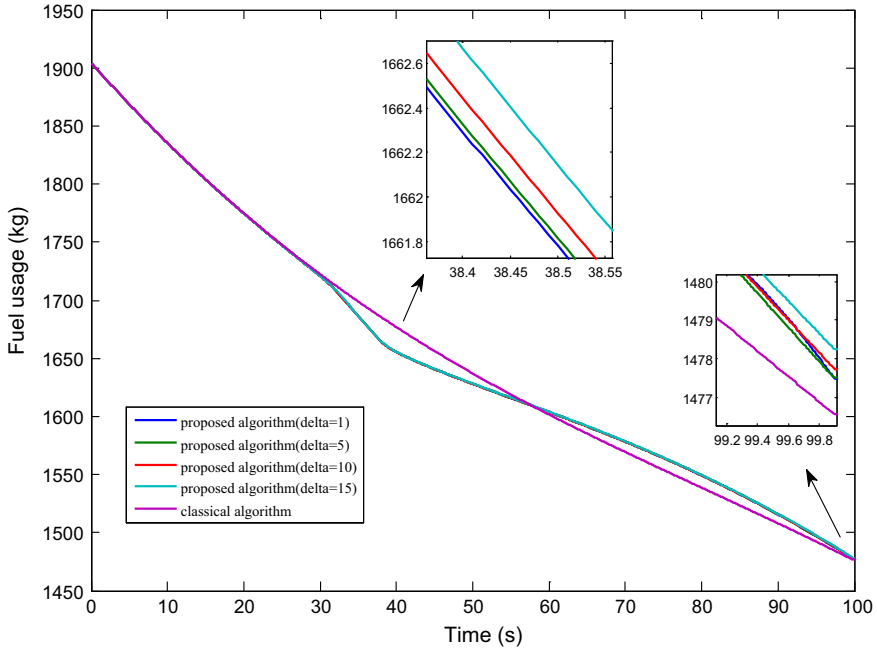

Fig. 17. Fuel usage under classical and proposed algorithms.

From Fig. 16 above, it can be seen that the proposed algorithm has good performance in avoiding collision. As the minimum safety distance δ becomes bigger, the minimum value along altitude axis of the trajectory is bigger, which means the lander has farther distance from Martian surface before landing on the target site. We can find in Fig. 17 that the additional term in the guidance to provide the collision avoidance capabilities does not significantly impact the fuel consumption, providing similar levels to that of the classical algorithm.

(3) The thruster constraint effect

In order to show the effect of the thruster constraint, the simulation is made here to illustrate certain range of parameters in the proposed guidance will make the collision avoidance guidance unsuccessful.

From Fig. 18 above, we can see that if c is chosen as a small value, although the terminal constraint is satisfied and the precision landing is guaranteed, the lander will crash on the Martian surface. The reason is that the value

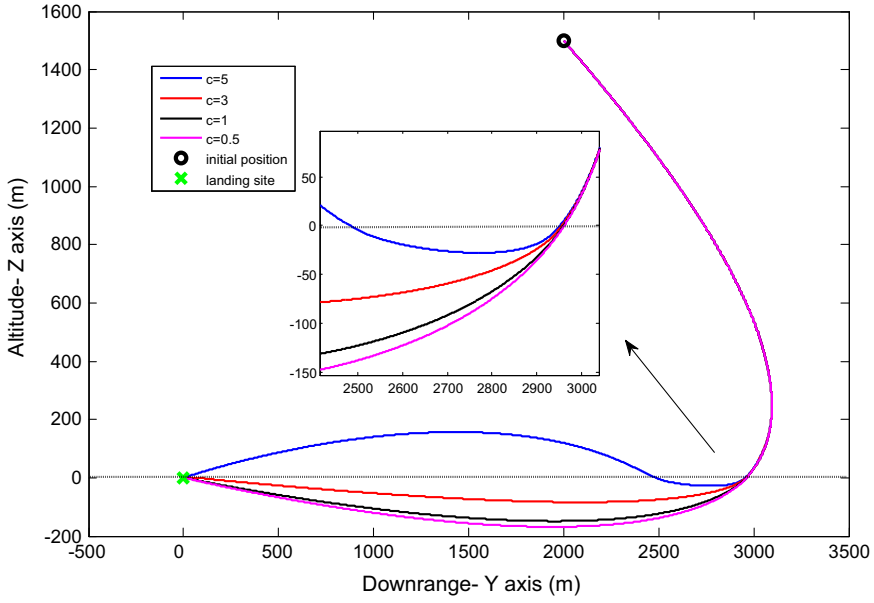

Fig. 18. Trajectories of the proposed algorithm under different value of c.

of $-\frac{c}{r_z^2+\varphi}\boldsymbol{Ar}$ in the performance index is expected to be minimized, which will make the value of $\boldsymbol{Ar}$ bigger as c is getting smaller, i.e. bigger command acceleration is added upwards, and it leads to the failure of avoiding collision due to the thruster constraint.

It can be found in Fig. 19 that if the value of δ is chosen as a big value, the collision avoidance mission will fail. Similar with Fig. 18, Fig. 19 illustrates that terminal constraint is satisfied as well as the need of precision landing. The reason can also be found by analyzing the term of $-\frac{c}{r_z^2+\varphi}\boldsymbol{Ar}$ in the performance index. When δ is set as a bigger value, φ will become bigger due to $\varphi = \delta^2/3$ in (13), which will make the value of $\boldsymbol{Ar}$ bigger, i.e. bigger command acceleration is added upwards in this situation to ensure a bigger value of $\boldsymbol{Ar}$, and if an outside-boundary command signal is needed to avoid collision, the thruster constraint will lead to the failure.

Therefore, it is necessary to find out the relationship between the best values of these parameters and the initial state of the lander. Here, we use $a_{\max z}$ to display the thrust constraint in the altitude direction, which denotes the maximum command acceleration can be provided by the lander, and $a_{\max z} > 0$. From the proposed performance index (13) and the proposed guidance (22), we can get Eq. (32), which can ensure the performance index is positive.

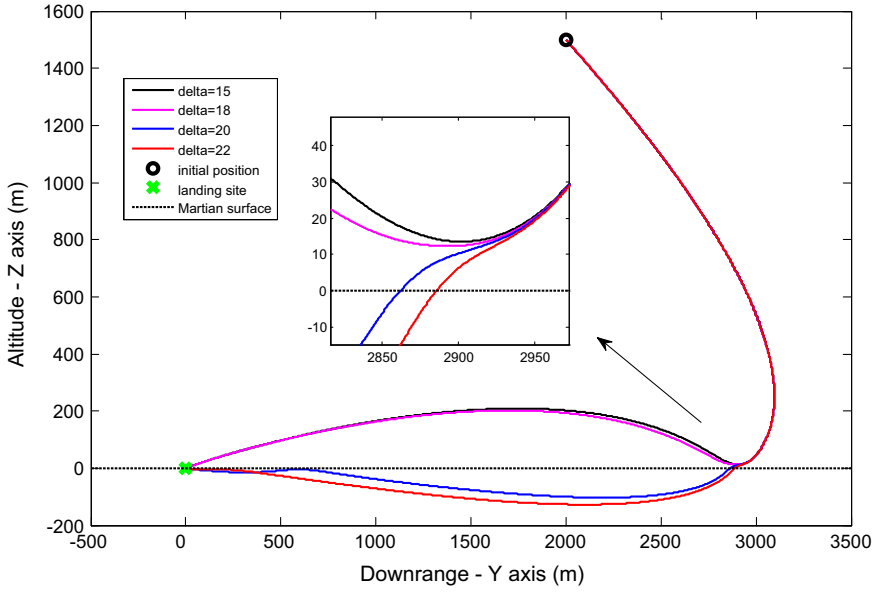

Fig. 19. Trajectories of the proposed algorithm under different value of δ.

$$a_{maxz}^2 - \frac{cr_z}{r_z^2 + \varphi} \geqslant 0 \tag{32}$$

There are many solutions of Eq. (32), and we set $r_z = \delta$ in order to increase the conservatism, and we can get

$$a_{\max z}^2 \geqslant \frac{3}{4} \cdot \frac{c}{\delta} \tag{33}$$

Note that the initial position and velocity of the lander will influence the trajectories definitely, so if we set $a_{\max z}^2 = \frac{3}{4} \cdot \frac{c}{\delta}$ and set the initial position as the most dangerous position, i.e. $r_z = \delta$, $v_z = 0$, then after substituting $a_{\max z}^2 = \frac{3}{4} \cdot \frac{c}{\delta}$ into the proposed guidance (34), we can obtain Eq. (35) below, which is a method to select these parameters conservatively.

$$a_z = -\frac{6r_z}{t_{go}^2} - \frac{4v_z}{t_{go}} - g + t_{go}^2 \cdot \frac{c}{24} \cdot \frac{r_z^2 - \varphi}{\left[r_z^2 + \varphi\right]^2} \tag{34}$$

$$-\frac{6\delta}{t_f^2} - g + t_f^2 \cdot \frac{1}{64} \cdot \frac{c}{\delta^2} \leqslant \sqrt{\frac{3}{4} \cdot \frac{c}{\delta}} \tag{35}$$

5. Conclusions

Collision avoidance ZEM/ZEV optimal feedback guidance has been proposed for the Mars powered descent phase, which has been proved effective in avoiding crashing the Martian surface by taking the altitude constraint into consideration. A term of collision avoidance was added in the performance index, which leaded to a new form of ZEM/ZEV guidance. Detailed information was expressed with analysis and derivation included. Simulation results confirmed the proposed algorithm and showed the parameters effect on the proposed algorithm. The research results can be applied to obstacle avoidance problems. Further study will mainly focus on the obstacle avoidance topic.

Acknowledgements

This work is supported by the National Natural Science Foundation of China (Grant Nos. 61174200, 61304005, 61403103), and the National Basic Research Program of China (2012CB720000). Many thanks to reviewers for their helpful comments.

References

Acikmese, B., Ploen, S.R., 2007. Convex programming approach to powered descent guidance for Mars landing. J. Guid. Control Dynam. 30 (5), 1353–1366.

Acikmese, B., Scharf, D., Blackmore, L., et al., 2008. Enhancements on the convex programming based powered descent guidance algorithm for Mars landing. AIAA J.

Blackmore, L., Acikmese, B., Scharf, D.P., 2010. Minimum-landing-error powered-descent guidance for mars landing using convex optimization. J. Guid. Control Dynam. 33 (4), 1161–1171.

Braun, R.D., Manning, R.M., 2007. Mars exploration entry, descent and landing challenges. J. Spacecraft Rock. 44 (2), 310–323.

Ebrahimi, B., Bahrami, M., Roshanian, J., 2008. Optimal sliding-mode guidance with terminal velocity constraint for fixed-interval propulsive Maneuvers. Acta Astronaut. 62 (s 10–11), 556–562.

Furfaro, R., Selnick, S., Cupples, M.L., et al., 2011. Non-linear sliding guidance algorithms for precision lunar landing. Adv. Astronaut. Sci. 140, 945–964.

Guo, Y., Hawkins, M., Wie, B., 2011. Optimal feedback guidance algorithms for planetary landing and asteroid intercept[C]. In: AAS/AIAA Astrodynamics Specialist Conference 2011, 2011–588.

Guo, Y., Hawkins, M., Wie, B., 2013a. Applications of generalized zero-effort-miss/zero-effort-velocity feedback guidance algorithm. J. Guid. Control Dynam. 36 (3), 810–820.

Guo, Y., Hawkins, M., Wie, B., 2013b. Waypoint-optimized zero-effort-miss/zero-effort-velocity feedback guidance for mars landing. J. Guid. Control Dynam. 36 (3), 799–809.

Johnson, A.E., Klumpp, A.R., Collier, J.B., et al., 2002. Lidar-based hazard avoidance for safe landing on mars. J. Guid. Control Dynam. 25 (6), 1091–1099.

Neveu, D., Lafontaine, J.D., Lebel, K., 2005. Validation of autonomous hazard-avoidance mars landing via closed-loop simulations. In: AIAA Modeling and Simulation Technologies Conference and Exhibit.

Rui, X., Cui, P., Xu, X., 2005. Realization of multi-agent planning system for autonomous spacecraft. Adv. Eng. Softw. 36 (4), 266–272.

Wells, G.W., Lafleur, J.M., Verges, A., et al., 2006. Entry descent and landing challenges of human mars exploration. Adv. Astronaut. Sci. 125.

Wibben, D., Furfaro, R., 2015. Optimal sliding guidance algorithm for Mars powered descent phase. Adv. Space Res. 57 (4), 948–961.

Wong, E.C., Singh, G., Masciarelli, J.P., 2002. Autonomous guidance and control design for hazard avoidance and safe landing on Mars. J. Spacecraft Rock. 43 (2), 378–384.

Zhou, L., Xia, Y., 2014. Improved ZEM/ZEV feedback guidance for Mars powered descent phase. Adv. Space Res. 54 (11), 2446–2455.